

# Atomic force microscopy measurements of crystal nucleation and growth rates in thin films of amorphous Te alloys

J. Kalb<sup>a)</sup> and F. Spaepen

*Division of Engineering and Applied Sciences, Harvard University, Cambridge, Massachusetts 02138*

M. Wuttig

*I. Physikalisches Institut der RWTH Aachen, 52056 Aachen, Germany*

(Received 6 February 2004; accepted 30 April 2004; published online 10 June 2004)

*Ex situ* atomic force microscopy in combination with a high-precision furnace has been employed for a systematic study of crystallization kinetics of sputtered amorphous  $\text{Ag}_{0.055}\text{In}_{0.065}\text{Sb}_{0.59}\text{Te}_{0.29}$ ,  $\text{Ge}_4\text{Sb}_1\text{Te}_5$ , and  $\text{Ge}_2\text{Sb}_2\text{Te}_5$  thin films used for optical data storage. Direct observation of crystals enabled us to establish the temperature dependence of the crystal nucleation rate and crystal growth velocity around 150 °C. While these alloys exhibited similar crystal growth characteristics, the crystal nucleation behavior of  $\text{Ag}_{0.055}\text{In}_{0.065}\text{Sb}_{0.59}\text{Te}_{0.29}$  differed significantly from that of  $\text{Ge}_4\text{Sb}_1\text{Te}_5$  and  $\text{Ge}_2\text{Sb}_2\text{Te}_5$ . These observations provide an explanation for the different recrystallization mechanisms observed upon laser heating of amorphous marks. © 2004 American Institute of Physics. [DOI: 10.1063/1.1764591]

A commercial medium of high potential for rewriteable data storage is based on phase change recording. In rewriteable (RW) compact disks and digital video disks (DVDs), a thin film of a Te alloy is locally and reversibly switched by laser heating between the amorphous and the crystalline state. These states can be distinguished optically by their difference in reflectivity.<sup>1</sup> For a high signal-to-noise ratio, a pronounced change in optical properties is essential, which requires a significant structural change. On the other hand, rapid switching between these states demands small atomic rearrangements. This remarkable combination of seemingly contrary properties is unique for Te alloys and is of high scientific and industrial interest. To meet future requirements for multi-media applications, the data transfer rate of phase change media must further be increased. This can only be achieved by accelerating the time-limiting factor, which is the recrystallization of an amorphous mark in crystalline surrounding. Therefore, it is essential to understand the mechanisms of recrystallization of phase change materials. Two mechanisms of recrystallization depending on the composition of the alloy have been observed. For instance, AgIn-doped  $\text{Sb}_2\text{Te}$  (the material of choice in DVD-RW) recrystallizes by the growth of the crystalline phase from the rim of the amorphous mark.<sup>2</sup> In contrast,  $\text{Ge}_4\text{Sb}_1\text{Te}_5$  and  $\text{Ge}_2\text{Sb}_2\text{Te}_5$  (the latter is the material of choice in DVD-random access memory) recrystallize by nucleation and subsequent growth of crystals inside the amorphous mark.<sup>3</sup> The atomistic basis for this difference is still not clearly understood. Even though several research groups have assumed that these alloys differ in their crystal nucleation rate and crystal growth velocity, systematic measurements of these two quantities as a function of temperature for *both* recrystallization mechanisms have to the best of our knowledge not been performed. Therefore, in many modeling studies of recrystallization, the fitting parameters have no direct experimental justification.<sup>4–6</sup> Additional difficulties arise because the glass transition temperature  $T_g$  is usually accompanied by a dis-

continuity in the temperature derivative of several physical quantities.<sup>7–9</sup> Therefore, crystallization parameters (in particular activation energies) determined experimentally from the easily accessible amorphous phase (below  $T_g$ ) cannot be extrapolated into the undercooled liquid (above  $T_g$ ). Only experimental data collected above  $T_g$  are useful for the simulation and understanding of the recrystallization process of phase change media under operating conditions. Therefore, there is a strong demand for systematic measurements of the nucleation and growth rates in the regime of the undercooled liquid.

Transmission electron microscopy (TEM) is a powerful tool to study crystallization of thin films of amorphous Te alloys.<sup>10</sup> Isothermal nucleation and growth rates as a function of temperature have been measured by *in situ* TEM for  $\text{Ge}_2\text{Sb}_2\text{Te}_5$  (Refs. 11 and 12) by counting crystals and measuring their change in size. This method, however, has two major uncertainties: First, precise temperature control (which is essential due to the strong temperature dependence of thermally activated processes) is often very difficult,<sup>11</sup> and second, the electron beam significantly influences crystallization.<sup>13,14</sup>

In this letter, we present a different approach to the determinations of nucleation and growth rates, which avoids these two difficulties. Due to the mass density increase upon crystallization, which induces a reduction in film thickness on the order of 5%,<sup>15,16</sup> crystals could be directly observed as depressions in the amorphous film with a Digital Instruments 3100 atomic force microscope (AFM) in TappingMode™. Three compositions,  $\text{Ag}_{0.055}\text{In}_{0.065}\text{Sb}_{0.59}\text{Te}_{0.29}$  (hereafter AgInSbTe),  $\text{Ge}_4\text{Sb}_1\text{Te}_5$ , and  $\text{Ge}_2\text{Sb}_2\text{Te}_5$ , were investigated. These films (thickness: 30 nm) were prepared by direct current magnetron sputtering on 640  $\mu\text{m}$  thick Si (100) wafers. The background pressure was approximately  $10^{-6}$  mbar and the working pressure during sputtering in Ar ambient was  $7 \times 10^{-3}$  mbar. The sputtering power was 100 W. The deposition rate was approximately 0.5 nm/s and the target-substrate distance 5 cm. As determined from x-ray diffraction (XRD) measurements, the structure of the as-deposited films was entirely amorphous, i.e., no evidence of partial

<sup>a)</sup>Also at: I. Physikalisches Institut der RWTH Aachen, 52056 Aachen, Germany; electronic mail: kalb@deas.harvard.edu

crystallization during deposition could be observed. These samples were alternately *ex situ* annealed and scanned in the AFM. A specific sample was always annealed at the *same* temperature and rescanned in the AFM at the *same* microscopic location (this was possible by scratching the film with a fine needle and using the optical microscope attached to the AFM to relocate the site). Using several samples, these annealing/rescanning cycles were performed at several temperatures, 5 °C apart (experimentally observable ranges: 140 °C–185 °C for AgInSbTe and Ge<sub>4</sub>Sb<sub>1</sub>Te<sub>5</sub>; and 115 °C–145 °C for Ge<sub>2</sub>Sb<sub>2</sub>Te<sub>5</sub>). The isothermal crystal growth velocity was determined from two subsequent AFM scans from the ratio of the increase in crystal radius (average over 10–20 crystals) and the annealing time. Depending on the temperature, between 2 and 9 annealing/rescanning cycles were performed. This enabled us to establish the time dependence of the growth velocity for up to eight stages of the transformation. Counting, as a function of time, the number of crystals per unit area gave the isothermal crystal nucleation rate.

For the lower temperatures, where crystallization proceeded on a time scale of hours to minutes, annealing was performed in a high-precision furnace of a Perkin–Elmer Pyris 1 differential scanning calorimeter (DSC) in an argon atmosphere [furnace dimensions: 9 mm diameter, 4 mm height (cylindrical), temperature uncertainty: Less than 0.1 °C, heating/cooling rate: 50 K/min, no overshoot]. For the higher temperatures, where crystallization proceeded on a time scale of about a minute to a few seconds, the sample was immersed manually into safflower oil of the desired temperature and subsequently quenched into room-temperature ethylene glycol. The sample (8 mm × 4 mm) was held by a copper wire (0.5 mm diameter), which was coiled two or three times around the sample. The oil was stirred continuously, and its temperature was measured by a mercury thermometer (temperature uncertainty: Less than 0.5 °C). Oil residues on the sample were cleaned off with an isopropanol-soaked soft cloth after each anneal.

Figure 1 shows a selection of two AFM scans for two temperatures per alloy. Scans on Ge<sub>4</sub>Sb<sub>1</sub>Te<sub>5</sub> and Ge<sub>2</sub>Sb<sub>2</sub>Te<sub>5</sub> look qualitatively similar. The scans on AgInSbTe differ from those on the GeSbTe alloys in two major respects: First, at a given time and temperature (represented by a single AFM scan), the crystal diameter distribution is rather sharp for AgInSbTe but broad for the GeSbTe alloys. Since the isothermal crystal growth velocity of neighboring crystals was observed to be identical, this implies that all (heterogeneous) nucleation sites are approximately simultaneously exhausted for AgInSbTe. In contrast, the isothermal nucleation rate remains nonzero at all times for the GeSbTe alloys. Second, the total number of crystals per unit area, which would be observed after complete crystallization of the sample surface, increases with increasing temperature for the GeSbTe alloys, but adopts a temperature-independent value of  $(5.0 \pm 0.3) \mu\text{m}^{-2}$  for AgInSbTe. This behavior was observed in the entire temperature range investigated. Cross-sectional TEM (Refs. 17 and 18) shows that crystals nucleate only heterogeneously at the (naturally oxidized) film surface. Heterogeneous nucleation at the film–substrate interface did not occur.

Over the entire temperature range investigated, the isothermal crystal growth velocity was observed to be time-independent for all three alloys. This implies that the growth

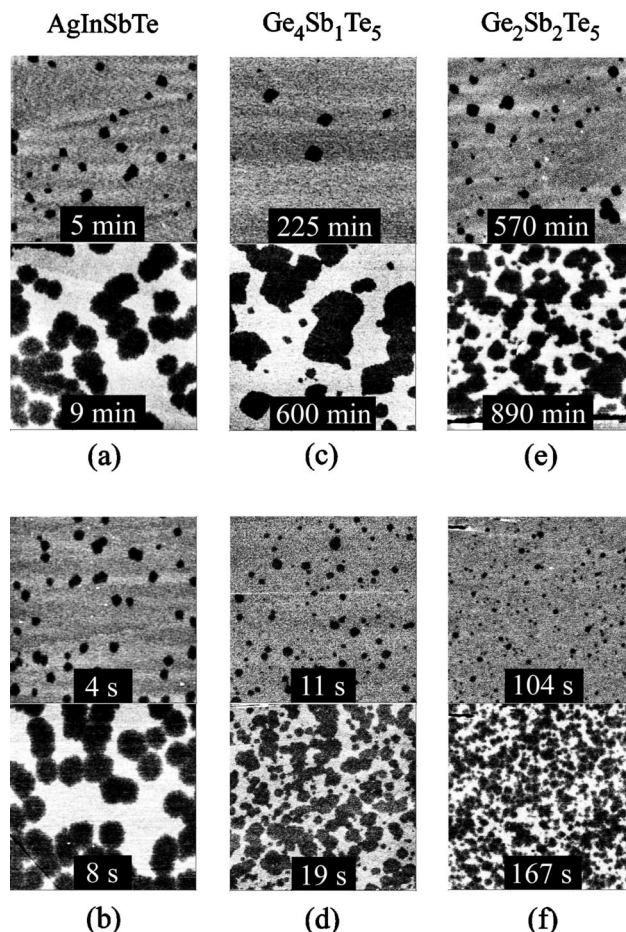


FIG. 1. AFM scans (dimensions: 3  $\mu\text{m}$  by 3  $\mu\text{m}$ ): Crystals (dark, height:  $-2$  nm) are visible in amorphous surrounding (bright, zero height): (a) AgInSbTe, 160 °C. (b) AgInSbTe, 185 °C. (c) Ge<sub>4</sub>Sb<sub>1</sub>Te<sub>5</sub>, 140 °C. (d) Ge<sub>4</sub>Sb<sub>1</sub>Te<sub>5</sub>, 180 °C. (e) Ge<sub>2</sub>Sb<sub>2</sub>Te<sub>5</sub>, 115 °C. (f) Ge<sub>2</sub>Sb<sub>2</sub>Te<sub>5</sub>, 145 °C. All times indicated are *total* times (including times of preceding anneals). Note that each crystal in (a) and (b) is present in both top and bottom images.

was interface-controlled (in contrast to diffusion-controlled growth, where the position of the interface is proportional to the square root of time).<sup>19</sup> Figure 2 is an Arrhenius plot of the crystal growth velocities,  $u$ . Growth velocities of AgInSbTe and Ge<sub>4</sub>Sb<sub>1</sub>Te<sub>5</sub> are similar at a given temperature. Crystal growth is thermally activated. The fitting parameters obtained from the Arrhenius fits are given in Table I. For Ge<sub>2</sub>Sb<sub>2</sub>Te<sub>5</sub>, our value of  $E_u = (2.35 \pm 0.05)$  eV agrees well with that of Privitera *et al.*<sup>12</sup> [ $E_u = (2.4 \pm 0.3)$  eV] but differs slightly from that of Ruitenbergh *et al.*<sup>11</sup> [ $E_u = (1.6 \pm 0.6)$  eV]. Both literature values were obtained in about the same temperature range by *in situ* TEM. The deviation between the latter value and ours may be due to the large temperature uncertainty of  $\pm 10$  °C reported in Ref. 11.

For all alloys,  $E_u$  is significantly higher than the value for the isoconfigurational viscosity,  $E_\eta$ , which was measured<sup>20</sup> between 60 °C and 100 °C (Table I). Since the transport coefficients for viscous flow, diffusion and crystal growth are proportional, their activation energies should be the same. However, as the glass transition temperature  $T_g$  is usually accompanied by a discontinuity in activation energies,<sup>7–9</sup> the data presented in Fig. 2 appear to be taken *above* the glass transition temperature  $T_g$ , that is, in the undercooled liquid state:  $T_g$  depends on the time scale of the experiment<sup>7–9</sup> and should be significantly lower in these iso-

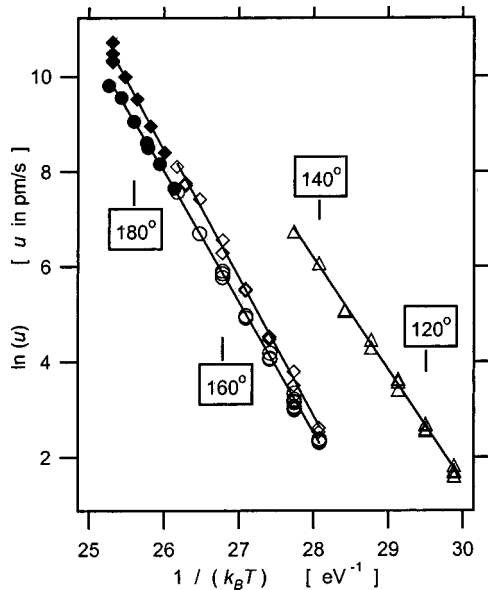


FIG. 2. Crystal growth velocity  $u$  as a function of temperature  $T$ . Open squares: AgInSbTe, DSC anneal. Full squares: AgInSbTe, Immersion anneal. Open circles: Ge<sub>4</sub>Sb<sub>1</sub>Te<sub>5</sub>, DSC anneal. Full circles: Ge<sub>4</sub>Sb<sub>1</sub>Te<sub>5</sub>, Immersion anneal. Open triangles: Ge<sub>2</sub>Sb<sub>2</sub>Te<sub>5</sub>, DSC anneal. For Ge<sub>2</sub>Sb<sub>2</sub>Te<sub>5</sub>, the crystal density was too high to allow measurements using immersion anneals. The error bars on the velocity are on the order of the symbol size. For AgInSbTe and Ge<sub>4</sub>Sb<sub>1</sub>Te<sub>5</sub>, DSC and immersion anneal data were fitted separately, and the fitting parameters were subsequently averaged. These averaged values (Table I) are less sensitive to possible small systematic errors in the temperature calibration of the two annealing methods.

thermal experiments than the values of  $T_g \sim 150^\circ\text{C} - 190^\circ\text{C}$  determined in the earlier scanning experiments.<sup>21</sup> In contrast, the measurements presented in Ref. 20 were performed far below  $T_g$  in the amorphous phase. That the crystal growth velocity in Fig. 2 is time-independent points in the same direction: Only in the amorphous phase, but not in the undercooled liquid, would a time dependence of the atomic transport rates be expected due to structural relaxation.<sup>8,9,20</sup>

In conclusion, we have demonstrated that the combination of an AFM and a high-precision furnace provides an accurate method to determine isothermal crystallization parameters as a function of time and temperature. Our method should be generally applicable to thin films that exhibit het-

TABLE I. Fitting parameters of the Arrhenius fits  $[\ln(u) = \ln(u_0) - E_u/(k_B T)]$  in Fig. 2. Activation energies for the isoconfigurational viscosity  $E_\eta$  are given for comparison.

Alloy	$\ln(u_0)$ ( $u_0$ in pm/s)	$E_u$ (eV)	$E_\eta^a$ (eV)
AgInSbTe	$84.0 \pm 1.2$	$2.90 \pm 0.05$	$1.33 \pm 0.09$
Ge <sub>4</sub> Sb <sub>1</sub> Te <sub>5</sub>	$79.2 \pm 0.8$	$2.74 \pm 0.03$	$1.94 \pm 0.09$
Ge <sub>2</sub> Sb <sub>2</sub> Te <sub>5</sub>	$72.0 \pm 1.5$	$2.35 \pm 0.05$	$1.76 \pm 0.05$

<sup>a</sup>From Ref. 20.

erogeneous crystal nucleation at the film surface and a density change upon crystallization of a few percent. The difference in nucleation behavior between AgInSbTe and the GeSbTe alloys was observed to be much more pronounced than the difference in growth characteristics (all three alloys exhibited interface-controlled growth and similar activation energies  $E_u$  between 2.3 and 2.9 eV). This suggests that the different recrystallization mechanisms observed upon laser heating<sup>2,3</sup> can be ascribed to the significant difference in crystal nucleation behavior rather than to the smaller difference in crystal growth velocity. The continuous nucleation observed in the GeSbTe alloys is reflected in the nucleation-dominated recrystallization of laser-heated amorphous marks;<sup>3</sup> the saturation of nucleation observed in AgInSbTe corresponds to the growth-dominated recrystallization of the marks.<sup>2</sup>

The authors thank H. Dieker for help with the sample preparation. One of the authors (J.K.) acknowledges the Deutscher Akademischer Austauschdienst and the Studienstiftung des Deutschen Volkes for financial support. Another author (F.S.) acknowledges partial support from the Alexander-von-Humboldt-Stiftung. Work at Harvard is supported in part by the MRSEC program of the NSF.

<sup>1</sup>N. Yamada, Mater. Res. Bull. **21**, 48 (1996).

<sup>2</sup>H. J. Borg, M. van Schijndel, J. C. N. Rijpers, M. H. R. Lankhorst, G. Zhou, M. J. Dekker, I. P. D. Ubbens, and M. Kuijper, Jpn. J. Appl. Phys., Part 1 **40**, 1592 (2001).

<sup>3</sup>J. H. Coombs, A. P. J. M. Jongenelis, W. van Es-Spiekman and B. A. J. Jacobs, J. Appl. Phys. **78**, 4918 (1995).

<sup>4</sup>C. Peng, L. Cheng, and M. Mansuripur, J. Appl. Phys. **82**, 4183 (1997).

<sup>5</sup>A. C. Sheila and T. E. Schlesinger, J. Appl. Phys. **91**, 2803 (2002).

<sup>6</sup>E. R. Meinders, H. J. Borg, M. H. R. Lankhorst, J. Hellmig, and A. V. Mijrskii, J. Appl. Phys. **91**, 9794 (2002).

<sup>7</sup>W. Kauzmann, Chem. Rev. (Washington, D.C.) **43**, 219 (1948).

<sup>8</sup>F. Spaepen, in *Physics of Defects*, edited by R. Balian, M. Kleman, and J.-P. Poirier, Les Houches Lectures Vol. 35 (North-Holland, Amsterdam, 1981), pp. 136–174.

<sup>9</sup>F. Spaepen and D. Turnbull, Annu. Rev. Phys. Chem. **35**, 241 (1984).

<sup>10</sup>M. Libera and M. Chen, J. Appl. Phys. **73**, 2272 (1993).

<sup>11</sup>G. Ruitenber, A. K. Petford-Long, and R. C. Doole, J. Appl. Phys. **92**, 3116 (2002).

<sup>12</sup>S. Privitera, C. Bongiorno, E. Rimini, R. Zonca, A. Pirovano, and R. Bez, Mater. Res. Soc. Symp. Proc. **803**, HH 1.4 (2004).

<sup>13</sup>M. Libera, Appl. Phys. Lett. **68**, 331 (1996).

<sup>14</sup>B. J. Kooi, W. M. G. Groot, and J. T. M. De Hosson, J. Appl. Phys. **95**, 924 (2004).

<sup>15</sup>V. Weidenhof, I. Friedrich, S. Ziegler, and M. Wuttig, J. Appl. Phys. **86**, 5879 (1999).

<sup>16</sup>T. P. Leervad Pedersen, J. Kalb, W. K. Njoroge, D. Wamwangi, M. Wuttig, and F. Spaepen, Appl. Phys. Lett. **79**, 3597 (2001).

<sup>17</sup>T. H. Jeong, M. R. Kim, H. Seo, S. J. Kim, and S. Y. Kim, J. Appl. Phys. **86**, 774 (1999).

<sup>18</sup>J. Kalb, C.-Y. Wen, F. Spaepen, and M. Wuttig (unpublished).

<sup>19</sup>J. W. Christian, *The Theory of Transformations in Metals and Alloys*, 2nd ed. (Pergamon, North-Holland, Amsterdam, 1975).

<sup>20</sup>J. Kalb, F. Spaepen, T. P. Leervad Pedersen, and M. Wuttig, J. Appl. Phys. **94**, 4908 (2003).

<sup>21</sup>J. Kalb, F. Spaepen, and M. Wuttig, J. Appl. Phys. **93**, 2389 (2003).